# NUMERICAL STUDY OF TEMPERATURE AND VELOCITY DISTRIBUTIONS IN MECHANICAL SEALS WITHOUT FLUSH FLOW USING UNSTRUCTURED GRID

*F. A. AlAwaidi*
***Mechanical Technology Department, Riyadh College of Technology***
General Organization for Technical Education and Vocational Training (GOTEVOT)
P.O. Box 32261 Riyadh 11428, Saudi Arabia
* awaidif@hotmail.com

## ABSTRACT

In this paper, numerical analysis of heat transfer problems in mechanical seals has been investigated by predicting the temperature and velocity distributions within the sealed fluid in the flow field above the inner cylinder of the mechanical seal. This prediction has been performed using FLUENT, a computational fluid dynamics computer program, which is, used for modeling fluid flow, heat transfer, and chemical reaction problems. Three-dimensional axisymmetric model has been developed which includes symmetrical inlet conditions of the fluid without flush flow. The results of a typical seal model have been computed and analyzed. The heat generation is distributed along the interface contact regions. Results using unstructured grid distribution in the heat generation region have been studied. This analysis is important since temperature changes greatly alter the seal geometry. At high temperatures the sealed fluid may become a vapor, and at high or low temperatures the seal materials may behave differently. This study will lead to a greater understanding of the behavior and performance of the mechanical seals by providing more knowledge of the entire seal thermal environment.

## NOMENCLATURE

| | |
|---|---|
| b | heat generation region length (m) |
| d | seal outside diameter (m) |
| N | rotational speed of the seal (rpm) |
| P | pressure on the sliding seal surface (MPa) |
| q | heat generation (W) |
| R | radius (m) |
| $S_\phi$ | general source or sink term for any dependent $\phi$ |
| T | temperature (K) |
| t | time (s) |
| u | x-direction velocity (m/s) |
| v | y-direction velocity (m/s) |
| V | heat generation volume ($m^3$) |
| (x,y) | rectangular (Cartesian) coordinates in 2-D |
| Y | radial direction |
| Z | axial direction |

**Manuscript received from Dr . F.A.Al Awaidi**
**Accepted on : 2 / 8 / 2003**
**Engineering Research Journal Vol 26, No 4, 2003 Minufiya University, Faculty Of Engineering , Shebien El-Kom , Egypt , ISSN 1110-1180**

**Greek Symbols**

$\phi$ general dependent variable (u, v, p , T, … etc.)

$\Gamma_\phi$ general exchange coefficient for any variable $\phi$

$\mu$ dynamic viscosity (kg/m-sec)

$\nu$ kinematic viscosity ($m^2$/s)

$\rho$ density (kg/$m^3$)

$\left.\begin{array}{l}\overline{\rho u'\phi'}\\ \overline{\rho v'\phi'}\end{array}\right\}$ Reynolds stress terms

**Superscripts**

$\overline{\phantom{x}}$ mean value of the variable

**Subscripts**

i inner

o outer

## INTRODUCTION

Seal technology plays a vital role in modern engineering technology because of the ever-increasing severity of industrial, military, and commercial requirements. In fact, the development of industrial rotating and reciprocating equipment is often limited by the reliability of the sealing devices employed. Figure 1 shows the heat transfer paths in a mechanical seal, [12]. Most of the heat is generated in the moving-fixed parts interface and must pass from the seal by conduction and convection to the sealed fluid.

Most of the heat generated at the seal interface is conducted away from the faces to other parts of the seal rings where it is then dissipated by convection. The conduction paths between the interface and the edges of the seal ring are very important to ensure proper cooling at the interface of the seal. Thermal conductivity of the seal parts materials is the most important variable in controlling the temperature difference across the conduction paths.

After heat is conducted away from the faces through the seal rings, most of the heat is then removed from the seal rings by convection heat transfer to the fluid surrounding the seal parts. This basic heat transfer process occurs regardless of how the surrounding fluid is cooled. The convection heat transfer coefficient is equal in importance to the thermal conductivity of the seal parts in determining the temperature rise.

Figure 1 also shows the possible heat sinks for the seal discussed in this paper. The heat generated at the seal interface heats the various seal parts that in turn heat the surrounding fluid, the shaft, and the seal housing. The fluid surrounding the seal slowly exchanges heat with the pumped fluid. The shaft and the housing may also transfer heat between the fluid surrounding the seal and the process fluid by serving as a conduction link in a convection – conduction – convection path. In any case, cooling by this way may be poor and the seal temperature could be very high.

Another method to provide good cooling to a seal is to by pass a small amount of flow from the pump discharge into the seal region by a flew passage as shown in Figure 1. This way of cooling is called flush cooling. The temperature can be controlled by using a heat exchanger and a separate cooling flow. The flush flow not only assures good cooling, but it also assures that a continued supply of clean fluid is present at the seal inlet side as opposed to what may simply accumulate in a dead-end chamber. The flush flow can also be separate clean fluid or filtered fluid. Thus, the flush flow can be used to control this important aspect of seal environment as well as the temperature.

The analysis of the heat transfer problem of mechanical seals was attempted on a two-dimensional model. But, according to Merati et al. [6], the flow inside the seal chamber is not symmetrical due to non-symmetrical inlet conditions in addition to the non-symmetrical behavior of the turbulent flow in the seal chamber due to the injection of a flush flow for removal of heat. So two-dimensional models are not descriptive enough to understand the thermal behavior of the mechanical seal.

A three dimensional model was developed by AL-Awaidy [3] using uniform and nonuniform grid distributions. Sanga [5] developed a similar model but it was concentrated on the computational and programming aspects more than the mechanical and thermal aspects. Also, Ref. [5] did not work with real dimensions, real fluid properties, and real boundary conditions. So, Ref. [5] gave a general idea about ideal seal behavior.

Pascovisci and Einstein [7] showed that various parameters are affecting the seal's thermal behavior. Ref. [8] states that an increase in the thermal conductivity of the rotor material means a more uniform radial temperature distribution. According to Ref. [9], a real mechanical seal model is needed to analyze and study the thermal distortions of the seal mating faces which affect the sealing performance.

One of the most important publications on mechanical seals was an analytical study of phase changes in mechanical face seals (when the fluid is liquid), carried out by Hughes, et al. [13]. It introduced a subject of great interest to seal designers as well as users, the effect of phase change across the seal face. This study was based upon certain assumptions. One of these assumptions was the leakage flow rate is small so that convective heat transport in the fluid may be neglected compared to the conduction into the seal faces became distorted. It is mentioned in Refs. [13] and [10] that the combination of pressure reduction and temperature increase across the sealing faces can cause the liquid to vaporize . The objective of this paper is to analyze the heat transfer problem in mechanical seals.

## MATHEMATICAL FORMULATION

The flow field to be analyzed is governed by the Reynolds averaged incompressible form of the Navier-Stokes equations. These equations are closed using the two-equation k-ε turbulence model. The equations are all similar and can be expressed into a common form as:-

$$\frac{\partial}{\partial t}(\rho\phi)+\frac{\partial}{\partial x}(\rho u\phi)+\frac{\partial}{\partial y}(\rho v\phi)=\frac{\partial}{\partial x}\left(\Gamma_\phi\frac{\partial\phi}{\partial x}-\rho\overline{u'\phi'}\right)+\frac{\partial}{\partial y}\left(\Gamma_\phi\frac{\partial\phi}{\partial y}-\rho\overline{v'\phi'}\right)+S_\phi \tag{1}$$

where the corresponding values for the exchange coefficient $\Gamma_\phi$ and the source or sink term $S_\phi$ for any variable $\phi$ are summarized in Ref. [4]. The Reynolds stresses $\rho\overline{u'\phi'}$ and $\rho\overline{v'\phi'}$ are related to mean flow quantities via k-ε turbulence models. The transport equations for this model have been discussed numerous times in the literature; therefore, that discussion will not be repeated here. The reader is referred to Ref. [4] for details.

The finite-volume method incorporated with the quadratic upwind interpolation scheme (QUICK) is employed to integrate and interpolate the partial differential equations represented by equation (1). The SIMPLEC, a variant of SIMPLE method developed by Patankar [11] was used to obtain the numerical solution of the discritized equations. Further details of the adopted numerical technique and its computer implementation is found in Ref. [4]. The computer program uses an Additive-Correction Multi-Grid procedure to accelerate the convergence of the standard line-by-line solver. In addition to solving the basic transport equations on the original fine-grid level, multi-grid techniques solve an equivalent equations set on each coarse grid level, transferring corrections onto the fine grid levels in an effort to achieve global balances and reduce the overall solution error. The use of multi-grid scheme can greatly reduce the number of iterations and the CPU time required to obtain a converged solution. The computations were performed on a 3600 unstructured grid nodes. The convergence criterion adopted in the calculations was set so that the normalized residual was less than $10^{-6}$ at any grid node and for any $\phi$ equation.

FLUENT provides more than one way to achieve the convergence of the solution. One of these ways is by turning off some parameters while continuing to calculate other parameters during calculation part. That is accomplished by first solving for the flow field without solving for the temperature or enthalpy. Once the pressure and velocity terms had converged or seem to be converged, the temperature options are turned on until the flow field had converged. The method currently used is to do the calculation part for all parameters together until the convergence satisfied.

## PHYSICAL MODEL & BOUNDARY CONDITIONS

In this paper, a typical seal model has been analyzed as shown in Figure 2. It was assumed that the cylindrical chamber was constructed using two concentric cylinders with inner cylinder rotating (the rotor, accessories, and shaft) and other stationary. One end of the cylindrical chamber was blocked off with a flat surface (the gland plate). It was assumed also that the outer boundaries of the housing were insulated. The fluid flows in and out in the axial direction. The working fluid in this study is water. The overall physical dimensions and quantities are provided by Durametalic Corporation.

In this model, heat is assumed to be generated in rotor and stator regions and is distributed uniformly through the primary seal components (rotor and stator). The values of the heat generation are computed using the following equation [9].

$$q = 2.44 * 10^{-3} * P^{0.67} * d^{1.8} * N^{0.8} \tag{2}$$

Heat generation values are entered into FLUENT as a volumetric heat generation. So, the volume of the heat generation region is needed and must be computed from the following equation:-

$$V = \pi (R_o^2 - R_i^2)\, b \tag{3}$$

FLUENT requires the user to input the turbulent intensity and charteristics length to determine the turbulence kinetic energy and eddy dissipation rate. Laser Doppler Velocimetry (LDV) results were used for turbulence intensity and for the inlet conditions of the fluid at different locations in the radial direction, [2]. Symmetrical inlet conditions were assumed which resulted in a two-dimensional problem only

For the numerical calculations, no-slip boundary conditions are used along the three walls. Constant heat flux boundary is used for the lower wall. The top and right walls are assumed to be adiabatic requiring the normal derivative of temperature to vanish. Along the fluid inflow boundaries, uniform conditions are used for both the velocity and temperature. At the outflow boundary, non-reflective boundary conditions are used where the boundary values were found by linear extrapolation from the interior points. Initial conditions are obtained by specifying free-stream conditions throughout the flow field.

## RESULTS AND DISCUSSION

In FLUENT, there are two methods to setup the problem. If the geometry which will be modeled has Cartesian (rectangular) or Cylindrical coordinates in either two or three dimensions (2D, 3D), it may be solved using FLUENT alone. For other geometries, preBFC can be used to setup the problem. In this paper, since the coordinates are cylindrical, FLUENT will be used to setup the geometry and grid. As mentioned before, since the inlet conditions are symmetric, it is better to do the complete analysis for 2-D problem to save time and efforts.

The results of this paper will compare two heat generation values, q=880 W and q=4120 W. To make this comparison possible, the same operating conditions are used for both cases. Water was used as the working fluid and its physical properties were used at room temperature for inlet boundary conditions. The fluid flows in and out in the axial direction equally as shown in Figure 2. Laser Doppler Velocimetry (LDV) results were used for inlet conditions of the fluid at different locations in the radial direction [2]. For both heat generation values, symmetrical inlet conditions were assumed. The total number of cells used is 3600 using unstructured grid distribution as shown in Figure 3. This grid distribution has been used for both heat generation values.

After specifying the coordinate system and the total number of cells used, the type of cells used should be specified to differentiate between inlets, outlet, and walls which have different physical conditions. In this paper, the flow calculations have taken place in the flow and interface regions only. The heat transfer in the gland plate, the shaft, and the accessories region will be studied in the future.

The velocity and temperature distributions for both heat generation values are given below. Figures 4 and 5 show the velocity distributions for both heat generations values, q = 880 W and q = 4120 W, at three radial direction locations in the flow region (Y= 0.004, 0.00825, and 0.012 m) respectively. All curves in these figures have the same characteristic shapes. The values of the velocity decrease rapidly to a certain extent. For q = 880 W, the velocity decrease rapidly until the middle of the flow region (Z $\approx$ 0.023 m). For q = 4120 W, the velocity decrease rapidly until near the middle of the flow region (Z $\approx$ 0.013 m) and a smooth decrease at Z $\approx$ 0.034 m. After that and for both heat generation values, the velocity decreases much slower until the end of the flow region (Z = 0.049 m). For both heat generation values, the maximum velocity was ranging from 0.6 to 0.65 m/s at the specified locations. Similar results were shown on the contours of the velocity magnitudes in Figure 8 for q = 880 W and in Figure 9 for q = 4120 W. These results show that as the heat generation value increases, the fluid returns back and leaves the flow region fast and this may be due to the diffusion of heat from heat generation region between the stator and the rotor.

The temperature distributions for both heat generations values, q = 880 W and q = 4120 W, at three locations in the radial direction above the inner cylinder (Y= 0.004, 0.00825, and 0.012 m) are shown in Figs. 6 and 7 respectively. For q = 880 W, the temperature curves increase rapidly until the end of the flow region. Differences in the temperature through the flow region are not big because of low heat generation value and the locations chosen in the radial direction. For locations near the heat generation region, it is expected that a higher temperatures values will be found.

The temperature curves for the heat generation value of q = 4120 W is shown in Fig. 7. These curves increase in two jumps. A rapid increase first at Z = 0.013 m and a smooth increase at Z $\approx$ 0.034 m. These two points are the same points as that mentioned with the decrease in the velocity values. The highest temperature and the largest temperature gradients were in the heat generation region which is the interface contact areas. In both directions (axial and radial), moving away from the heat generation region towards the flow region or the shaft region, the temperature values decrease and the temperature gradients become flatter .

Differences in the temperature curves through the flow region for q = 4120 W showing the effect of higher heat generation value and the locations chosen in the radial direction. Again, for locations near the heat generation region, it is expected that a higher temperatures values will be found. This is clear from the temperature value at Y = 0.004 m the nearest point to the heat generation region as Z ranging from 0.041m to 0.049 m. The temperature values at these locations range from 309 K to 313 K for the specified radial locations above the inner cylinder at Y = 0.004, 0.00825, 0.012 m respectively. So it could be said that the highest temperature and the largest temperature gradients are located in the heat generation region.

As shown in Figures 6 and 7, high temperature values near the heat generation regions indicates the need for more cooling rate in these regions. This could be accomplished by studying the real models with and without flush flow.

Similar results were shown by the contours of the temperature distribution in Figure 10 for q = 880 W and in Figure 11 for q = 4120 W. These results show that as the heat generation value increases, the fluid temperature increases and reach its maximum value near the heat generation region between the stator and the rotor.

## CONCLUSIONS AND RECOMMENDATIONS

The prediction of temperature and velocity distributions within the sealed fluid at different locations in the radial direction above the inner cylinder of a typical mechanical seal is performed. This prediction has been done by using FLUENT, a computational fluid dynamics computer program which is used for modeling fluid flow, heat transfer, and chemical reaction problems. In actual seal, the heat is generated at the interface region. To satisfy this condition, it was assumed that the heat generation distributed along the interface contact region.

It was found that the highest temperature and the largest temperature gradients were in the heat generation region which is the interface contact areas. In both directions, moving away from the heat generation region towards the flow region, the temperature values decrease and the temperature gradients become flatter.

Using different heat generation values, a similar velocity distribution has been observed. It was inferred that the convection due to rotation dominates over that due to axial velocity. This is because the heat flux in the radial direction is less than in the axial direction.

In addition to the temperature and velocity distributions, the heat flux and the heat transfer coefficient should be investigated near the sliding surfaces.

It is recommended to predict the temperature distribution of various seal parts in order to asses the effect of temperature on materials and to find extent of distortion of the seal caused by non uniform temperatures. This investigation should be done using real mechanical seal case with and without flush flow. This study of the heat transfer problem in and around the heat generation region should include the shaft, stator, rotor, gland plate, and the accessories in addition to the flow region as shown in Figure 2. This objectives will be achieved by considering the real dimensions, properties, boundary conditions of the seal components and by the use of the flow software computer program – FLUENT

According to Merati et al. [1], Taylor-Couette flow is expected when a fluid with high viscosity has been used in the rotation of a cylinder within a concentric cylindrical cavity. So it is recommended to investigate a fluid with a higher viscosity.

Through this paper, it was assumed that the fluid properties are constant with temperature. According to Pascovisci and Einstein [7], assuming constant fluid properties, especially viscosity, along the radial width of the sealing dam can result in an unacceptable over estimation of the temperature. This should be achieved by studying the mechanical seal with material and fluid temperature dependent properties.

## REFERENCES


1. Merati, P., Phillips, R.L., DePayva, J.,"Effect of Impeller Geometry, Rotational Speed, and Fluid Properties on Seal Chamber Flow," 56th STLE Annual Meeting, Orlando, Florida, May 20-24, 2001, Tribology Transactions, Vol. 44, No. 3, pp. 451-457, July 2001.
2. Phillips, R. L., Merati, P., Jacobs, L.E., "Experimental Determination of the Thermal Characteristics of a Mechanical Seal and its Operating Environment, "52nd STLE Annual Meeting, Kansas City, Missouri, May 18-22,1997, Tribology Transactions, Vol. 40 , pp. 559-568, 1997.
3. AL-Awaidy, F., "Analysis of Heat Transfer Problems in Mechanical Seals," Project Report, Western Michigan University, 1994.
4. Fluent User's Guide V 4.2, Fluent Inc., New Hampshire, 1993.
5. Sanga, S., "Prediction of Temperature and Velocity Distribution in the Mechanical Seal Chamber," Western Michigan University, 1993.
6. Merati, P., Parker, I. C., and Adams, W. V., "Turbulent Flow of Annulus With Rotating Cylinder and Dead End Wall," Thirteen Symposium on Turbulence at Rolla, Missouri,, September 21-23, 1992.
7. Pascovisci, M. D., and Einstein, I., "A Thermo-Hydrodynamic Analysis of a Mechanical Face Seals," Journal of Tribology, Vol. 114, pp 639-648, 1992.
8. Lebeck, Alan O., "Principles and Design of Mechanical Face Seals," John Wiley & Sons, Inc., NewYork, 1991.
9. Merati, P., William, V., Ralph, P., and Robert, L., "Measurement and Prediction of Heat Transfer Coefficients for Mechanical Seals," Western Michigan University, 1991.
10. Buck, G. S., "A Methodology for Design and Application of Mechanical Seals," ASLE Trans., Vol. 23, No. 3, pp 244-252, 1980.
11. Patankar, S. V., "Numerical Heat Transfer and Fluid Flow," Mc-Graw Hill, NewYork, 1980.
12. Buchter, H. Hugo, "Industrial Sealing Technology," John Wiley & Sons, Inc., NewYork, 1979
13. Hughes, W. F., Winowich, N. S., Burchak, M. J. and Kenedy, W. C., "Phase Change in Liquid Face Seals," Jour. Of Lubr. Tech., Vol. 100, pp 74-79, 1978.

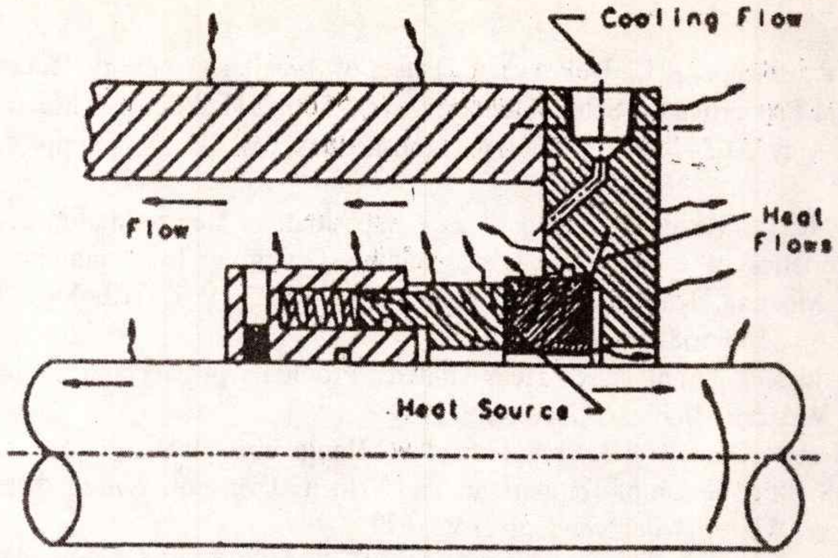


Fig. 1 The heat transfer paths in a mechanical seal.

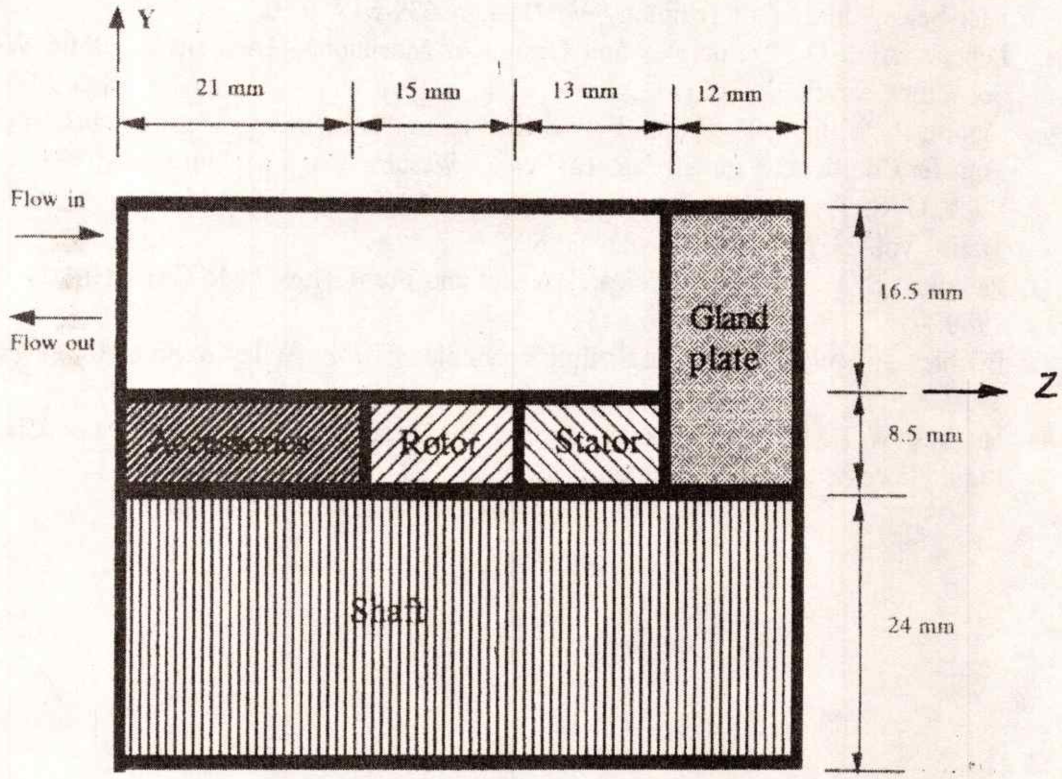


Fig. 2 Typical seal model without flush flow.

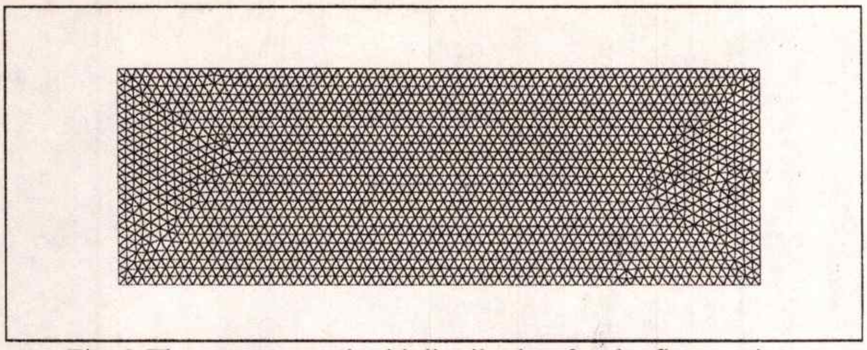

Fig. 3 The unstructured grid distribution for the flow region.

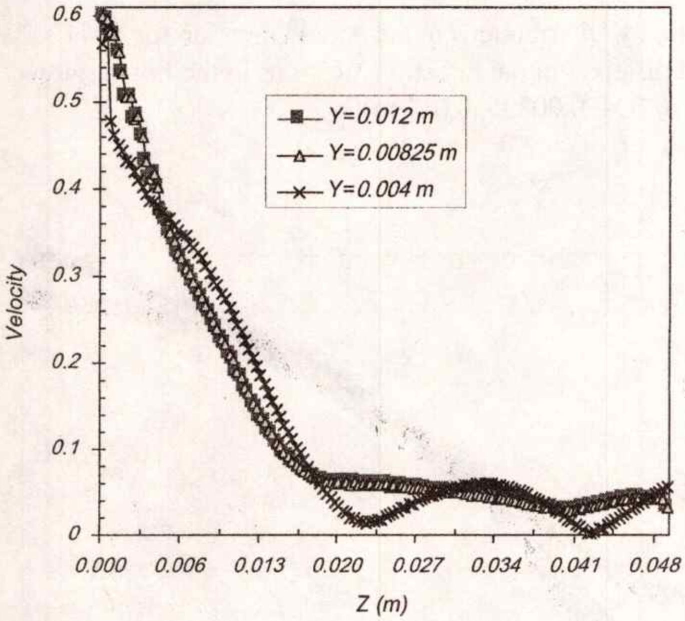


Fig. 4 Velocity Distributions in the Axial Direction for q=880 W
(at different radial direction locations in the flow region
Y=0.004, 0.00825, 0.012 m)

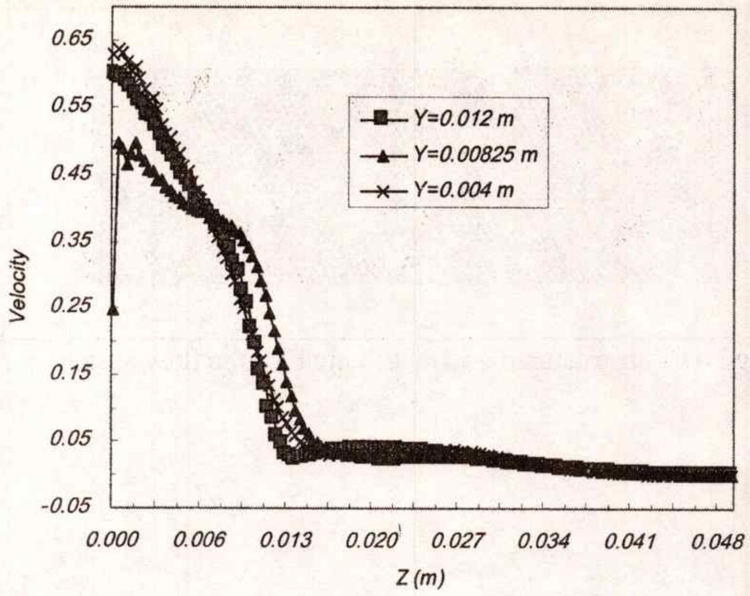


Fig. 5 Velocity Distributions in the Axial Direction for q=4120 W
(at different radial direction locations in the flow region
Y=0.004, 0.00825, 0.012 m)

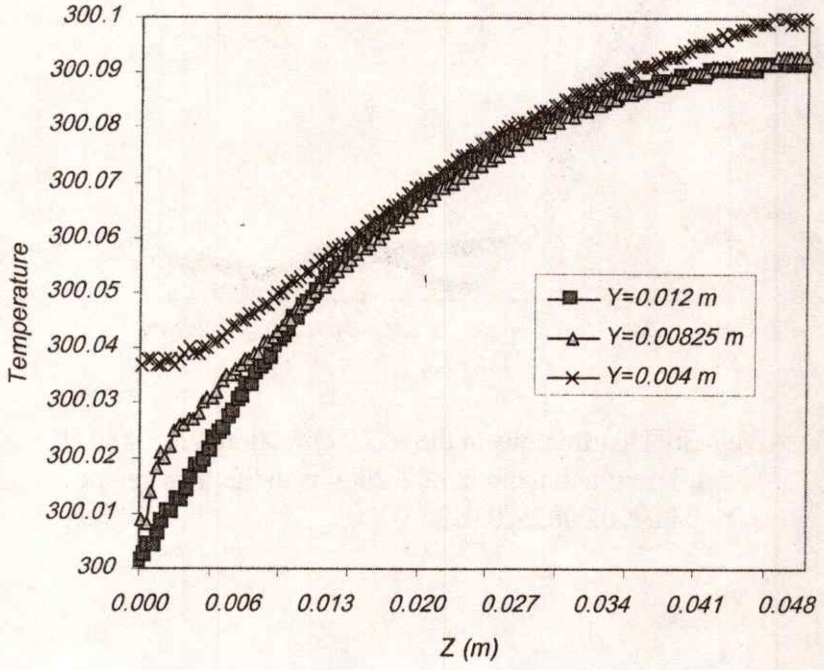


Fig. 6 Temperature Distributions in the Axial Direction for q=880 W
(at different radial direction locations in the flow region
Y=0.004, 0.00825, 0.012 m)

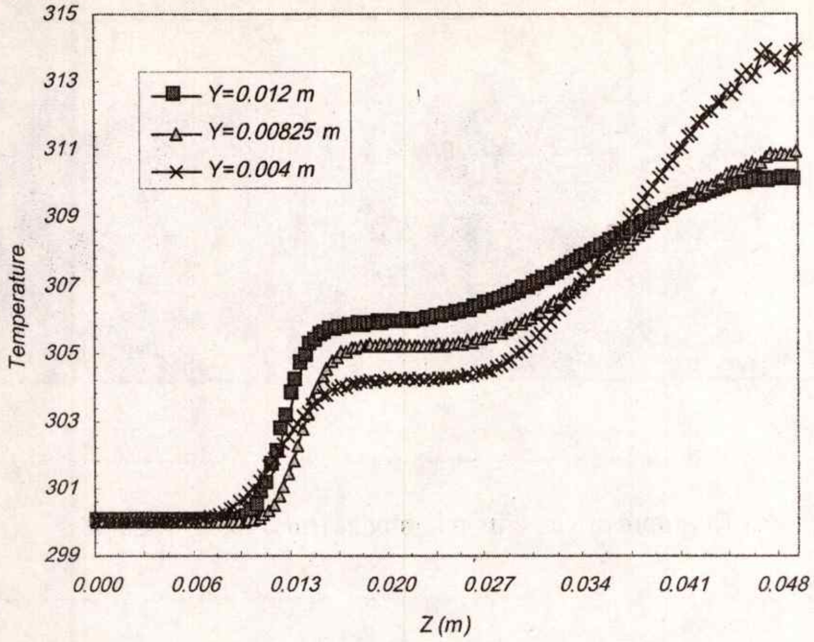


Fig. 7 Temperature Distributions in the Axial Direction for q=4120 W (at different radial direction location in the flow region Y=0.004, 0.00825, 0.012 m)

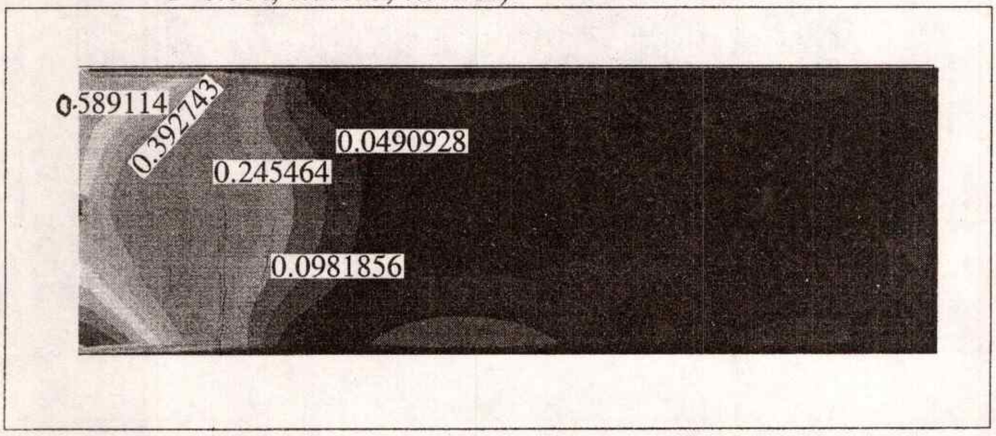


Fig. 8 Contours of velocity magnitudes (m/s) for q=880 W.

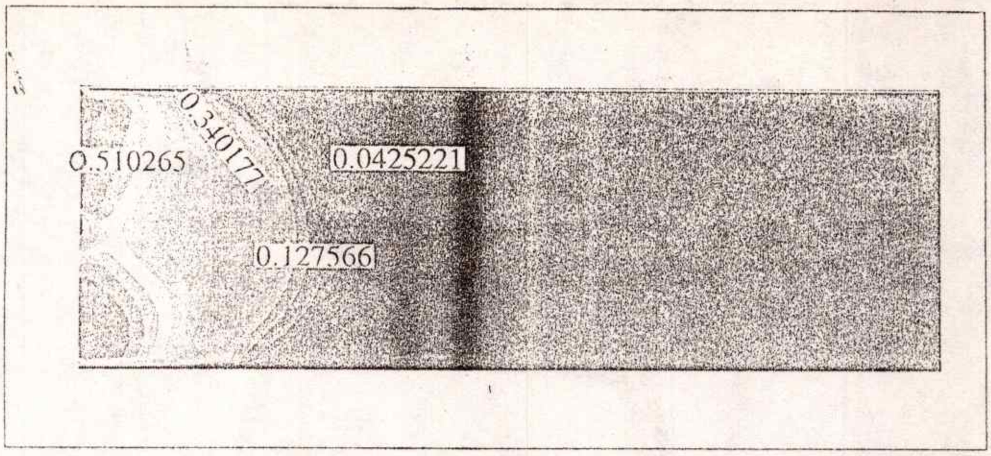


Fig. 9 Contours of velocity magnitudes (m/s) for q=4120 W.

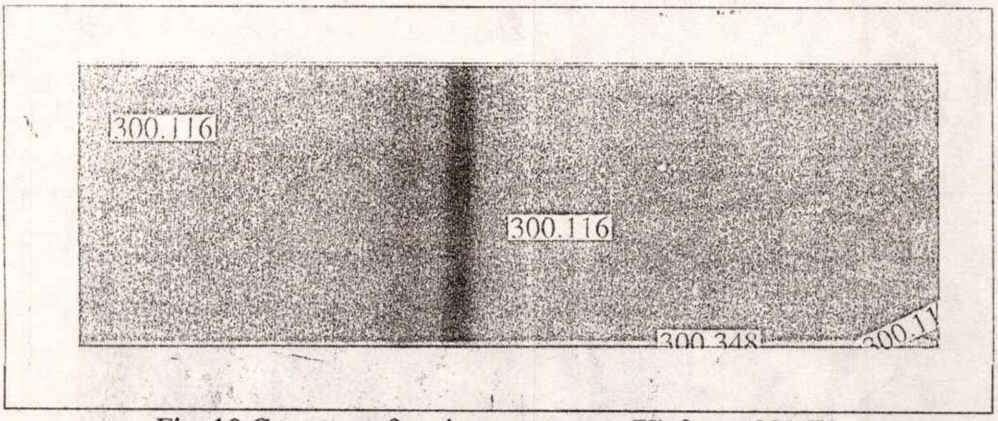


Fig. 10 Contours of static temperature (K) for q=880 W.

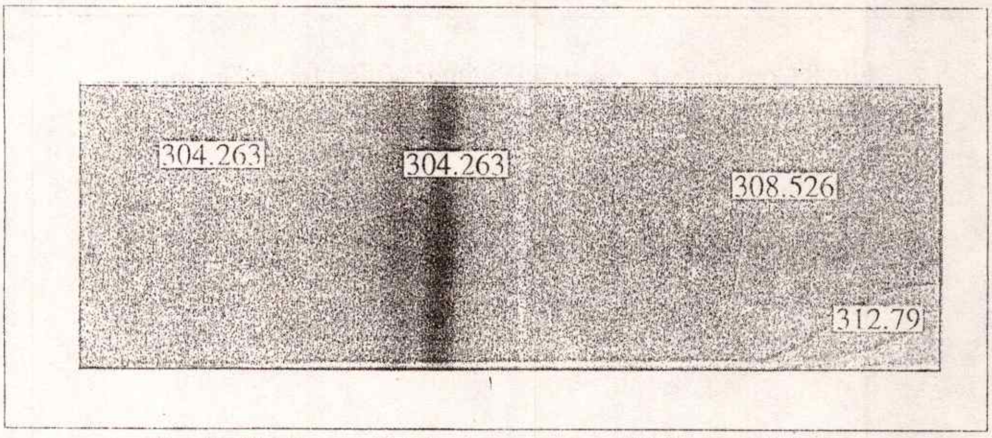


Fig. 11 Contours of static temperature (K) for q=4120 W.